Transcrystallinity Effects in High-Density Polyethylene. I. Experimental Observations in Differential Scanning Calorimetry Analysis

N. Billon, V. Henaff, E. Pelous, J. M. Haudin

Centre de Mise en Forme des Matériaux, UMR CNRS 7635, Ecole des Mines de Paris, BP 207, 06904 Sophia-Antipolis Cedex, France

Received 9 May 2001; accepted 20 December 2001

ABSTRACT: The crystallization of a high-density polyethylene was analyzed with differential scanning calorimetry (DSC) measurements. An intense transcrystallinity was observed at the contact between the polymer and the DSC pans. The modification of the crystallization kinetics induced by this phenomenon was studied as a function of cooling rate and sample thickness. We point out that most of the theoretical predictions of our previous model could be checked. The crystallization temperature was a function of the sample thickness and could be also correlated with the thickness of the transcrystalline zones. The shapes of the DSC traces were complex and correlated with the amount of trancrystallization. The usual interpretations of such DSC curves were not accurate. We conclude that specific experimental procedures must be proposed to understand and correctly use such measurements. © 2002 Wiley Periodicals, Inc. J Appl Polym Sci 86: 725–733, 2002

Key words: crystallization; transcrystallinity; kinetics (polym.); high-density polyethylene (HDPE); differential scanning calorimetry (DSC)

INTRODUCTION

The origin of this article was the common observation that some commercially available polymers develop intense transcrystalline regions when they are in contact with foreign bodies.[1–10] This phenomenon results from an important nucleation ability of the surfaces, which leads to the appearance of numerous additional nuclei. When it occurs during differential scanning calorimetry (DSC) analysis,[7,8,10] at the contact between polymer and pans, measurements are strongly disturbed. Then, such measurements are no longer representative of the polymer itself, and the data deduced from the analysis may be inaccurate for the characterization of the material because the DSC traces result from the competition between two physical processes: bulk nucleation, which is an intrinsic property of the material, and the transcrystallinity effect, which is a property of the surface or the interface. Of course, to characterize the polymer, only the former phenomenon must be taken into account. A previous work[10] found that transcrystallinity was so important that the intrinsic characterization of the crystallization kinetics of the polymer was impossible without a theoretical analysis.

Correspondence to: N. Billon (noelle.billon@cemef.cma.fr).

Journal of Applied Polymer Science, Vol. 86, 725–733 (2002)

At this stage, two solutions may be envisaged: first, to modify the experimental technique to get more significant results and, second, to develop theoretical and experimental procedures able to take trancrystallization into account. Obviously, the thinner the sample is, the higher the relative importance of the disturbing surface effects will be. So, the use of thick samples could make the problem negligible or, at least, less important.[9] Unfortunately, because of the low thermal conductivity of polymers, small samples must be used. Modifying the nature of the contact at the sample surfaces could be a pleasant solution to avoid transcrystalline zones. However, as the exact cause of trancrystallization is often unknown, it is still difficult to propose efficient surface modifications. In our laboratory, attempts to use molding agents were often unsuccessful.

So, it seems difficult to modify the experimental procedure in order to avoid, or at least to lower the effect of trancrystallization. Therefore, it is necessary to combine experimental procedures with appropriate theoretical analysis, which enables us to take into account trancrystallinity. To be efficient, the model has to be as simple as possible. Some potential routes were proposed in the past.[10] Unfortunately, the polyamide that was used exhibited a nonreproducible bulk nucleation. So, it was difficult to draw precise conclusions. In this work, we chose a polymer exhibiting important transcrystallinity phenomena in a much more reproducible way than the previous polyamide.

TABLE I
Values of the Sample Thicknesses

Mean value (μm)	Minimum value (μm)	Maximum value (μm)
192	182	203
315	305	336
510	492	525
651	622	671
865	849	885

We performed experiments, first, to study the polymer's sensitivity to transcrystalline effects and, second, to propose a procedure for the determination of the kinetic parameters for each of the involved phenomena: bulk crystallization and trancrystallization.

EXPERIMENTAL

The experiments were conducted with a high-density polyethylene (HDPE) grade (Eraclear IC 940 M) supplied by Enichem Polymres France. Its main characteristics are (1) average molecular weights: number-average (M_n) = 10,800, weight-average = 39,000, and z-average (M_z) = 98,400 and (2) density = 0.9574 g/cm^3.

The pellets were melted first for 5 min at 180°C between two glass slides on a Mettler FP 52 hot stage and then crystallized in air. This enabled us to obtain films of calibrated thickness. Disk-shaped specimens (diameter = 6 mm) were cut off from these films and introduced into aluminum DSC pans. Five different sample thicknesses were studied, whose mean values were 192, 315, 510, 651, and 865 μm, respectively (Table I).

The DSC samples were rapidly heated in a PerkinElmer DSC-7 calorimeter to a temperature of 180°C, where they were held for 5 min. Then, crystallization experiments were performed under 18 different constant cooling rates ranging from 0.3 to 50°C/min.

Calibration of the DSC apparatus has to be very rigorous to take into account internal thermal resistance and gradients. This was performed with pure In and Zn samples. In our case, temperature calibration was performed at a cooling rate of 10°C/min. In case the cooling rate was different from 10°C/min, the measured temperatures were systematically corrected to account for the cooling rate. This correction was determined experimentally with a set of measurements performed on pure In. By doing this, we took into account the thermal resistance between the DSC apparatus and the aluminum pans. Using flat samples and promoting a good mechanical contact between the material and the pans minimized additional thermal resistance between the pans and the polymer. In any case, the protocol for preparing the sample was as cautious as possible. The pans were systematically flattened before measurement, and base line was calibrated at any cooling rate.

The samples were removed and replaced after each crystallization. Microtomed cross-sections were cut from all the samples and observed by transmission optical microscopy between crossed polarizers with a Reichert Zetopan-Pol microscope. The cuts were 8 μm thick.

DSC traces recorded during cooling represented the evolution of heat flow versus time. They were numerically integrated, which led to an estimate of crystallization enthalpy. At each time, partial integrals were divided by enthalpy, which led to the evolution of the average mass-transformed fraction. In parallel, dividing heat flow by the enthalpy gave access to the derivative of the average transformed fraction with respect to time. Finally, these data were divided by the cooling rate. All these manipulations kept both the general shapes of the thermograms and the temperatures unchanged. The only aim was to "normalize" the peaks, that is, to make them have equivalent height whatever the cooling rate was. Additionally, we represented them versus temperature to draw them in the equivalent x axis. All treatments were made with a computer in a as precise as possible way.

Crystallization kinetics was then characterized with the shape of the thermograms, crystallization enthalpies, crystallization temperatures (chosen at the maximum of the DSC peaks), and onset temperatures (at which crystallization started).

RESULTS

General considerations

A lot of work was first devoted to the determination of the precision of the measurements. In contrast with the polyamide studied before,[10] this polymer exhibited a very reproducible behavior from one sample to another. With our experimental procedure, the dispersion on the crystallization temperature remained lower than ±1°C. In the same way, for a given thickness and cooling rate, the global shape (shoulder, location of the shoulder, etc.) of the thermograms and the morphologies of the samples were identical.

Crystallization kinetics

All the crystallization thermograms exhibited a complex shape with a shoulder. For samples with the same thicknesses, this shape significantly varied with the cooling rate (Fig. 1). As a whole, the crystallization trace shifted toward higher temperatures and was narrower when the cooling rate decreased. At high cooling rates a small shoulder was observed in the high-temperature region. Its relative importance

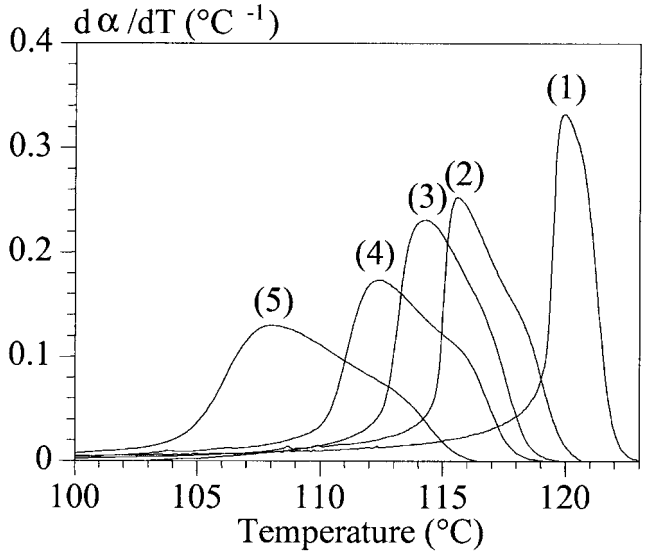

Figure 1 Experimental crystallization of approximately 192 μm thick samples: evolution of $d\alpha/dT$ versus temperature for five cooling rates: (1) 0.5°C/min and 194 μm, (2) 5°C/min and 200 μm, (3) 10°C/min and 189 μm, (4) 20°C/min and 191 μm, and (5) 50°C/min and 203 μm.

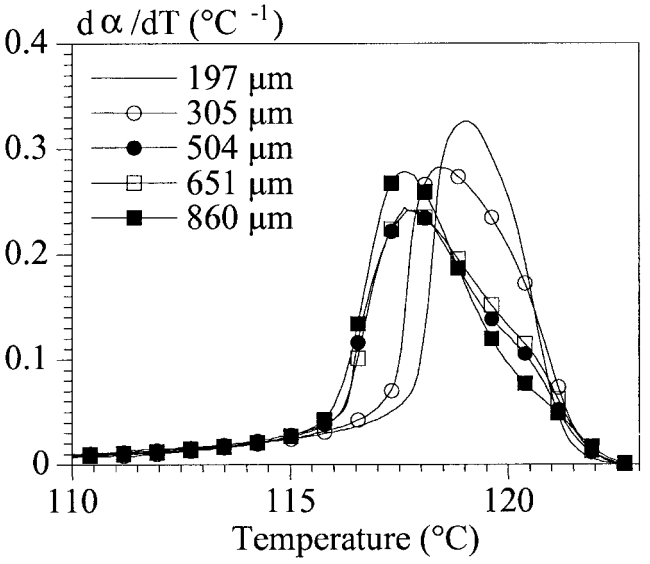

Figure 3 Experimental crystallization at a cooling rate of 1°C/min. Evolution of $d\alpha/dT$ versus temperature for five sample thicknesses: 197, 305, 504, 651, and 860 μm.

seemed to increase when the cooling rate decreased (Fig. 1). In fact, the main peak and the shoulder were closer, so that one seemingly tended to a single-peak situation (see the curve at 0.5°C/min, corresponding, in fact, to the superposition of two equivalent peaks very close to each other).

In parallel and for experiments performed at the same cooling rate, the relative importance of the shoulder seemed to increase when the thickness of the sample decreased (Fig. 2). This effect depended on the cooling rate (Figs. 2 and 3). Crystallization at low cooling rates was less sensitive to the thickness of the sample. Nevertheless, the beginning of the transformation occurred at similar temperatures, whereas the crystallization temperature (defined at the maximum of the main peak) could be significantly lowered when the thickness increased (Fig. 4). These temperatures did not decrease linearly. They tended to reach a plateau for high thicknesses. In conclusion, the shape of DSC traces and the crystallization temperature were very sensitive to the geometry of the sample, and the higher the cooling rate was, the more important the effect of the thickness was (Figs. 2–4).

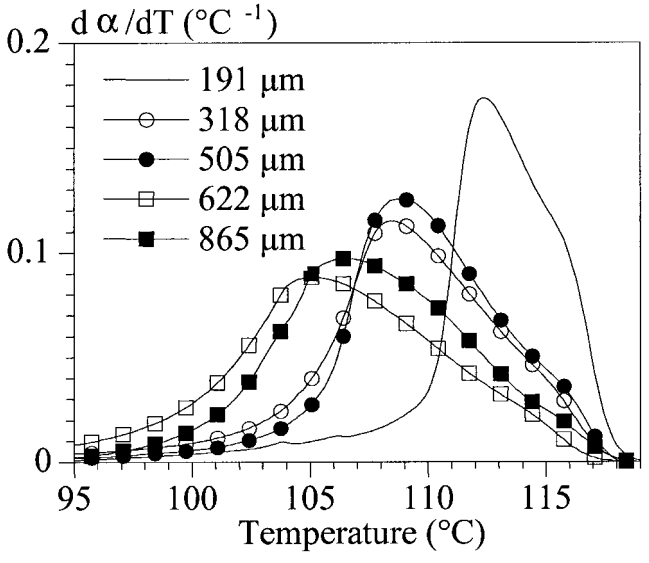

Figure 2 Experimental crystallization at a cooling rate of 20°C/min. Evolution of $d\alpha/dT$ versus temperature for five sample thicknesses: 191, 318, 505, 622, and 865 μm.

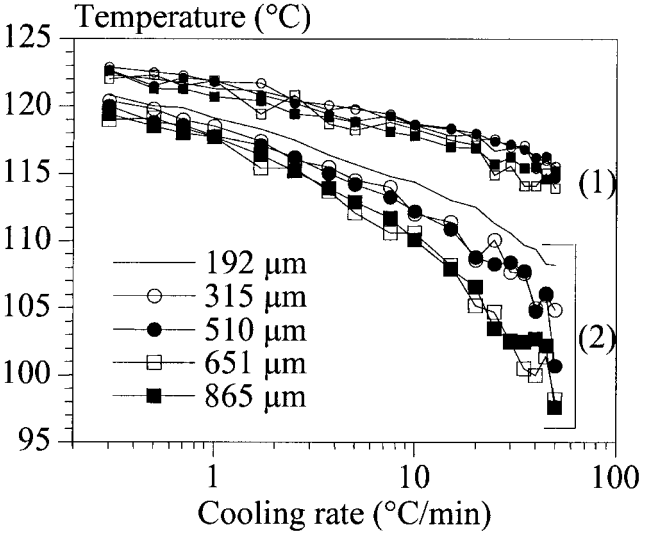

Figure 4 Experimental evolution of the (1) onset and (2) crystallization temperatures versus cooling rate for the five mean thicknesses studied.

TABLE II
Value of n as a Function of the Thickness of the Sample

	Mean thickness (μm)				
	192	315	510	651	865
n	3	2.7	2.85	2.7	1.82

The determination was performed for α ranging from 0.1 to 20%.

For its part, enthalpy of crystallization did not significantly vary with thickness or cooling rate. In 111 measurements, it ranged from 180 to 274 J/g, with a mean value of 236 J/g.

In summary, this HDPE exhibited complex crystallization kinetics, which were sensitive to the thickness of the sample, whereas its global crystallinity remained constant. The thinner the sample was, the higher the apparent crystallization temperature and the more important the effects were.

Obviously, such a behavior cannot be described with the classical description for overall crystallisation kinetics (e.g., ref. [11]):

$$\alpha = 1 - \exp\left(-\frac{\chi(T)}{|T_p|^n}\right) \quad (1)$$

where α is the transformed volume fraction; χ is a function of the temperature, T; T_p is the cooling rate, and n is the so-called Avrami exponent. n and the χ function depended on the thickness of the sample (Table II). They also depended on the range of α that was taken into account for their determination. For example, for the 192 μm thick samples, n was equal to 3.04 for transformed volume fractions ranging from 0.1 to 10%, whereas its value was 1.01 between 15 and 30%. It was difficult to draw any significant dependence of n versus the thickness and the transformed volume. Moreover, it was impossible to get a set of parameters, n and χ, able to entirely describe our experimental data. Obviously, it has been frequently observed that such a simple fitting is not totally pertinent, especially when integer n values are expected. Such effects of the thickness of the sample are, for their part, rarely reported. Numerous controversial articles concerning the Ozawa (or Avrami) approach exist. It could be tempting to simply argue that eq. (1) is not correct. It was demonstrated, however, that these approaches are rigorous from a mathematical point of view[12] and that very often discrepancy between the model and theory arises from the physical simplification involved in theories, that is, having only one type of nuclei uniformly distributed in the melt.

Microscopic observations

All the samples were cut and observed. They all exhibited important transcrystalline zones on their surfaces. Their morphology did not depend on the cooling rate but largely depended on sample thickness.

TABLE III
Comparison Between the Thickness of the Samples, the Thickness of the Transcrystalline Zones and the Maximum Diameter of the Spherulites

Mean thickness of the sample (μm)	Thickness of one transcrystalline zone (μm)	Mean maximum diameter of spherulites (μm)
192	93	95
315	127	143
510	150	212
651	180	268
865	161	293

The mean sizes of transcrystalline zones and the maximum diameter of the bulk spherulites were measured. They both increased as the thickness increased (Table III) up to a maximum value, which was nearly 350 μm (this value corresponded to the two transcrystalline zones). Both reached their maximum for the same sample thickness. It was possible to correlate the crystallization temperature with the thickness of the transcrystalline zones (Fig. 5).

Thin samples were nearly entirely overlapped by transcrystalline regions (Fig. 6). Medium-thickness samples (Figs. 7 and 8) contained more spherulites in their volume (bulk spherulites). Nevertheless, one "row" of spherulites to a maximum appeared in the midplane of these samples. Thick samples (Fig. 9), for their part, contained almost twice as many spherulites in the part of their thickness that was not overlapped by transcrystalline zones. So, up to a sample thickness of 510 μm, transcrystalline thickness was mainly limited by the sample thickness. In return, the growth of

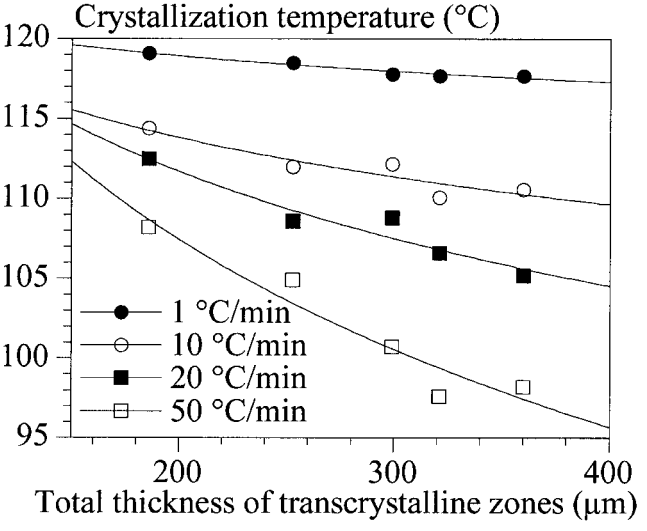

Figure 5 Experimental evolution of the crystallization temperature versus the thickness of the transcrystalline zones for four cooling rates.

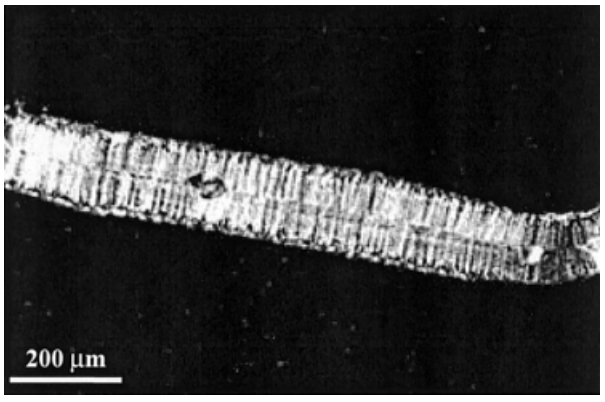

Figure 6 Morphology in the thickness of a DSC sample. The actual thickness of the sample was 182 μm. The cooling rate was 15°C/min.

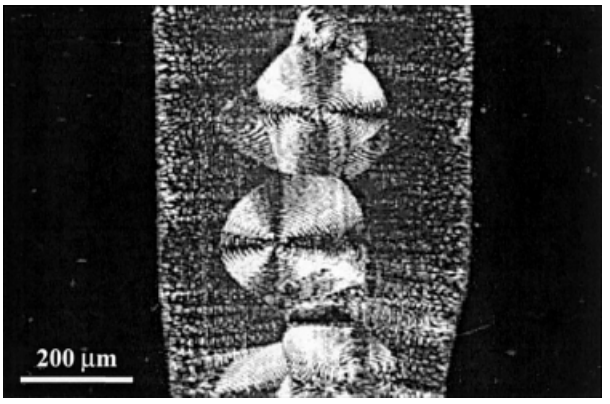

Figure 8 Morphology in the thickness of a DSC sample. The actual thickness of the sample was 519 μm. The cooling rate was 2.5°C/min.

coarse spherulites was constrained by transcrystallinity. Conversely, for thicker samples, transcrystallinity was stopped by coarse spherulites, which could, on average, grow without constraint. In these conditions, the diameter of coarse spherulites and transcrystalline thickness reached a plateau, and a further increase in the dimension of the sample resulted in an increase of the number of bulk spherulites.

DISCUSSION

Morphology

Observations and previous work[1–6] have shown that transcrystalline zones result from numerous nuclei located close to or at the surfaces of the sample. They promote spherulites that exhibit a quasi unidimensional growth due to their proximity. In our case, no morphological difference was observed between bulk spherulites and those located in the transcrystalline zones (except their sizes). This suggests that growth phenomena are identical and that transcrystalline zones and bulk polymers differ only in their nucleation processes. So, transcrystalline zones are caused by an important nucleating ability (at least higher than the ability of bulk nuclei) of DSC pans. This nucleating ability of aluminum, or more likely of alumina (Al_2O_3), has already been reported for various polymers.[5–8] In particular, in the case of polyethylene, this was also reported for DSC analysis.[7,8]

The final morphology of the polymer results from the competition between bulk and surface nucleation, as suggested for polypropylene[9] and demonstrated with experimental data on polyamide 6–6.[10] The more numerous the spherulites in the volume are, the lower the relative importance of the transcrystalline zones will be. This means that the fraction of the sample overlapped by transcrystalline zones decreases as the number of bulk nuclei increases.[9,10] This can be caused by an increase of either the nuclei density (due, for instance, to a nucleating agent) or the thickness of the sample. In this latter case, due to the fact that the activation of the transcrystalline zones seemingly takes place in the early stage of the transformation, transcrystalline regions may entirely transform thin

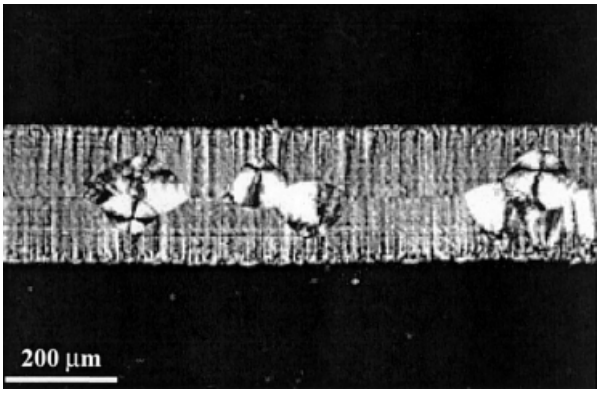

Figure 7 Morphology in the thickness of a DSC sample. The actual thickness of the sample was 318 μm. The cooling rate was 20°C/min.

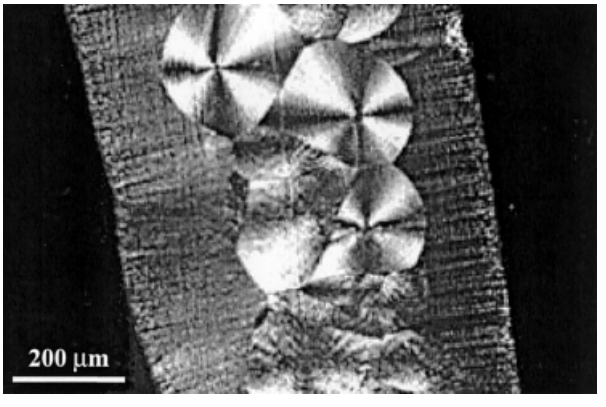

Figure 9 Morphology in the thickness of a DSC sample. The actual thickness of the sample was 857 μm. The cooling rate was 7.5°C/min.

samples before the activation of bulk nuclei. Because the growth rate of transcrystalline spherulites has a finite value, the thicker the sample is, the longer the time is given to bulk nuclei to be activated before they are overlapped by transcrystalline zones. So, in thick samples, nuclei in the midzone have more time to be activated than those in thin samples and, as a consequence, are more numerous. In return, these spherulites limit the growth of transcrytalline zones. Our experimental results are in good agreement with this description (Figs. 6–9 and Table III). In thin samples, the dimension of the transcrystalline region is limited by the thickness of the sample, and the inner spherulitic morphology is disturbed by transcrystallinity. The higher the thickness of the sample is, the more important the transcrystalline zones are, up to a certain value. Then, in thick samples, bulk spherulites are more numerous, and the dimension of the transcrystalline regions remains constant. As observed previously,[10] the mean diameter of spherulites is of the same order of magnitude as the thickness of the transcrystalline zones (Table III).

DSC traces

The DSC traces obtained in this study were already observed with polyamide 6-6 and correlated with the relative importance of transcrystalline zones.[10] A flatter complex shoulder-shaped peak was correlated with a thick transcrystalline region and few large coarse spherulites, whereas a single and higher crystallization peak corresponded to a thin transcrystalline zone and a large amount of small bulk spherulites.

These results are in agreement with the earlier ones. Once again, it was possible correlate the shapes of the peaks with the morphologies of the samples. Looking at Figures 2 and 4, it seems that samples can be classified into three groups: 192, 315–510, and 651–865 μm thick samples, respectively. The morphologies allowed the same classification: 315 and 510 μm thick samples were very similar, whereas 651 μm thick samples were similar to 865 μm thick ones. So, the relative importance of the shoulder was correlated to the level of constraint imposed to bulk nucleation in the midzone of the sample. No bulk nucleation corresponded to a trace associated with our thinnest sample (191 μm in Fig. 2), constrained bulk nucleation corresponded to our intermediate observation (318 μm in Fig. 2), and "free" bulk nucleation corresponded to our thickest sample (865 μm in Fig. 2).

Obviously, these modifications of crystallization temperature could partly be due to thermal gradients. First, recall that thermal resistance within the DSC apparatus was accounted for through a rigorous calibration. So, the only possible disturbance could result from the thermal gradient within the thick samples.[13] This effect could not be avoided. The use of thin samples could only minimize it. In our case, this effect could be neglected for samples thinner than 600 μm, especially for lower cooling rates (see Appendix).

In the previous work,[10] due to the nonreproducible behavior of the polymer, it was impossible to draw any founded conclusion concerning the correlation between cooling rate, DSC traces, and morphology. For this polyethylene and the experimental range explored in this study, we conclude that cooling rate does not significantly modify the morphology, even if the shape of the DSC peak is disturbed. This does signify that morphology is not sensitive to cooling rate or, in other terms, that the DSC traces are more sensitive to the cooling than global morphological observations, performed after the end of the crystallization experiment.

Using a theoretical approach,[12,14–17] which was an extension of Evans' theory,[18] we were able to develop a specific model to take into account transcrystallinity.[10] This model, coupled to computer simulations, allowed us to predict the effect of transcrystallinity and to reproduce experimental results concerning the shapes of DSC traces and their correlation with morphology.[10,19] It was established that the maximum of the peak is correlated with bulk nucleation even if, for a given bulk nucleation, it is shifted toward a higher temperature by trancrystallization, whereas the beginning of the peak is mainly related to transcrystallinity. Results depicted in Figures 2 to 4 confirm these points. First, shoulder-shaped peaks were observed in any cases in parallel with important transcrystalline zones. Second, when the amount of volume crystallization increased with the sample thickness, the maximum of the peak was shifted toward a lower temperature, whereas the beginning of the peak remained at temperatures similar to those observed for totally transcrystalline samples (191 μm in Fig. 2, 192 μm in Fig. 4).

Moreover, for given bulk and surface nucleation, the model[10] predicted that the crystallization temperature depends on sample thickness and that the higher the cooling rate is, the higher the predicted decrease in the crystallization temperature will be. Finally, as observed with this HDPE, calculations allowed us to predict a complex dependence versus thickness for n when transcrystallinity existed.[14,16]

In summary, most of our results confirm, in a qualitative way, the results of theoretical models that take into account transcrystalline zones, that is, complex shapes for the DSC traces, the dependence of crystallization temperature versus cooling rate, an abnormal n, and morphology evolution. In conclusion, as the experimental dispersion observed here was low, it would be interesting to use these results to extract data characterizing both phenomena, bulk and surface nucleations, on the basis of our previous theoretical analysis.[10]

CONCLUSIONS

The crystallization of a HDPE was studied with DSC analysis at constant cooling rates ranging from 0.3 to 50°C/min. Contact with DSC pans induced important transcrystalline zones on both sizes of the samples during cooling. Transcrystalline thickness was controlled either by the thickness of the sample, with thin samples, or by volume nucleation, in the case of thicker samples. Calorimetric measurements coupled with microscopic observations of the morphology of all the samples unambiguously confirmed the influence of trancrystallization on DSC measurements, as described previously.[10,19] The crystallization traces were always shoulder-shaped peaks. Measurements performed for different sample thicknesses, ranging from 192 to 865 μm, confirmed that the beginning of the transformation was mainly representative of trancrystallization. The main peak, for its part, was more sensitive to bulk crystallization.

From a practical point of view, we demonstrated that when trancrystallization occurs, DSC measurements are clearly dependent on the thickness of the sample, or more precisely, on the relative amount of transcrystalline zones. This is obviously generally not taken into account when DSC analysis is used to characterize polymer crystallization. As the DSC technique is difficult to modify to physically avoid trancrystallization, it is now necessary to develop a new method to analyze DSC curves. As experimental dispersion is weak for this polymer, it would be possible to extract accurate nucleation parameters from these experiments with simple models proposed elsewhere,[10] provided that the DSC apparatus was well calibrated. This is the scope of the following article.[24]

APPENDIX: COMPARISON OF RESPECTIVE EFFECTS OF THERMAL GRADIENT ACROSS THE SAMPLE AND TRANSCRYSTALLINITY IN DSC MEASUREMENTS

Introduction

To verify the foreseeable influence of thermal gradient inside the sample, we performed calculations. Equivalent crystallization conditions were chosen. Then, theoretical effects of trancrystallization without gradients were compared to theoretical effects of thermal gradients without transcrystallinity. Calculations were performed in conditions as close as possible to the actual conditions discussed in this article. Effects of transcrystallinity were modeled with our general model.[10,19] Obviously, in both cases α varied within the thickness of the polymer, and to model DSC measurements, we averaged it. The film was supposed to have infinite lateral dimensions, a finite thickness (e), and to be in contact with cooled aluminum pans. Due to our cautious protocol, the thermal resistance between the pans and the polymer were neglected.

Choice of an equivalent crystallization kinetics

A fictitious crystallization was built up to simulate a kinetics equivalent to that of our polyethylene, that is, equivalent crystallization temperatures and heat flowrates during cooling. Within the frame of Kolmogoroff–Avrami–Evans (KAE) analysis,[12,21] we chose to describe crystallization by the activation of potential nuclei distributed within the volume and by the growth of isotropic spherulites. The density of potential nuclei in the volume was 10^{-7} μm^{-3} and for convenience, nucleation was assumed to be instantaneous (as often in industrial polymers). The final average diameter of spherulites would be close to 260 μm, that is, of the same order of magnitude as the ones observed in the polymer we studied. The growth rate (G, in μm/s) was assumed to obey.[7,22,23]

$$G = 288.1 \exp\left(\frac{-28{,}202}{T(404 - T)}\right) \qquad \text{(A.1)}$$

with T in degrees Kelvin. We chose the numerical values to lead to a correct mathematical fit for G; they are discussed in the following article.[24] Transcrystallinity was modeled by the instantaneous nucleation of 6×10^{-4} nuclei μm^{-2} at the sample surface.[24]

Effect of trancrystallization

Temperature was assumed to be homogeneous within the thickness of the polymer. The sample was cooled down at a constant cooling rate, as the experiment was perfect. As reported previously,[10] the calculation enabled us to reproduce shoulder-shaped peaks. The crystallization temperature, chosen at the maximum of the peak of $d\alpha/dT$, decreased with increasing sample thickness and with increasing cooling rate (Fig. A.1). This evolution was in good qualitative agreement with our experimental observations (Fig. 4).

Effect of the thermal gradient

To evaluate the effect of the thermal gradient inside the sample during DSC analysis, we modeled the cooling of a thin film of polymer, solving the energy equation:[20]

$$\frac{\partial T(x,t)}{\partial t} - \left[\frac{k}{\rho C_p}\right]\frac{\partial^2 T(x,t)}{\partial x^2} = \left(\frac{\Delta H_a}{C_p}\right)\frac{\partial \alpha(x,t)}{\partial t} \qquad \text{(A.2)}$$

where x is the coordinate of a given point within the sample thickness and t is the time. k, ρ, C_p, and ΔH_a are the thermal conductivity, density, specific heat, and actual specific enthalpy of crystallization of the polymer, respectively. The surfaces of the polymer were in contact with metallic parts (here, aluminum), whose temperature was supposed to be controlled, and were

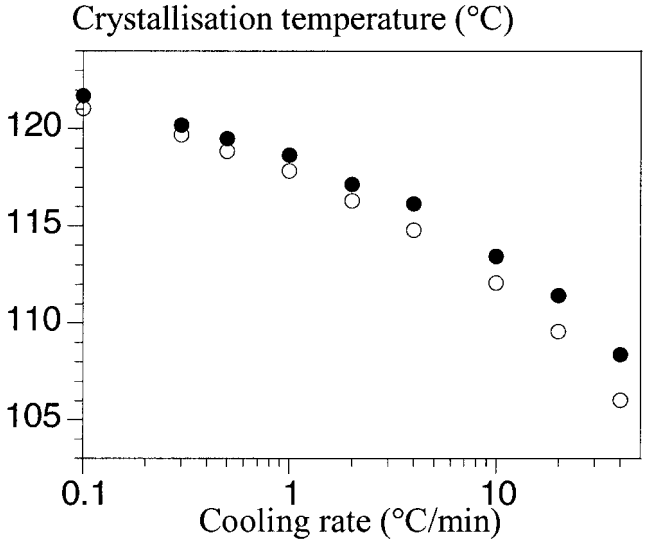

Figure A.1 Crystallization temperature versus cooling rate in (●) a 200 μm thick and (○) a 860 μm thick sample in the presence of transcrystallinity (no thermal gradient).

cooled down at a constant rate. The contact between polymer and metal was assumed to be perfect. The temperature of the polymer at the surface, T_s was given by

$$T_s = \frac{b_{al}T_{al} + b_{pol}T_{pol}}{b_{al} + b_{pol}} \quad (A.3)$$

where b $[(k\rho C_p)^{0.5}]$ is the thermal effusivity, T is the temperature, and al and pol refer to the metal and polymer, respectively. α was modelled with an extension of Ozawa's equation developed to describe any nonisothermal crystallization.[12,14,17,20] This model depends on two parameters: the Avrami exponent n, taken equal to 3, and the Ozawa parameter χ. In our case, to get crystallization kinetics equivalent to our fictitious case, this parameter was approximated by

$$\chi(T) = \exp(1.7 \times 10^5 - 1374\,T + 3.63\,T^2 - 0.003\,T^3) \quad (A.4)$$

where T is expressed in degrees Kelvin. In addition, k = 0.31 W/m K, ρ = 957.4 kg/m^3, C_p = 2717 J/kg K, b_{al} = 5852 J/m^{2}K s$^{0.5}$, and ΔH_a = 200 kJ/kg.

Numerical resolution was achieved with an explicit finite difference scheme.

This model is obviously not a complete model for DSC. It only aims at estimating the relative influence of the thermal gradient in the sample and transcrystallinity. If gradient in the sample is not negligible, the core temperature of the sample is higher than the surface temperature. As when DSC is well calibrated, the measured temperature is the surface temperature, measurement will underestimate the actual polymer temperature. Finally, in our case, the thermal gradient never induced shoulder-shaped peaks.

Discussion

As expected, the effect of the thermal gradient inside the sample increased as the cooling rate increased and as the thickness of the sample increased (Fig. A.2). However, the effects were negligible for thin samples at any cooling rate (used here) and at low cooling rates for our thicker samples. Conversely, trancrystallization always induced important disturbing effects.

The main difference between the two disturbing effects was visible and could be experimentally observed at low cooling rates: the effects of the thermal gradient disappeared, whereas those of trancrystallinity were still sensible. This was more clearly demonstrated by the evolution of the ratio, D (Fig. A.3), defined as

$$D = \frac{\text{Crystallization Temperature (°C) of a 200 } \mu\text{m Thick Sample}}{\text{Crystallization temperature (°C) of a 860 } \mu\text{m Thick Sample}} \quad (A.5)$$

At low cooling rates, the limiting value of this ratio was 1 in the case of the thermal gradient in the polymer, whereas it was higher than 1 in the case of transcrystallinity.

The shape of the experimental evolution of the crystallization temperature was closer to that predicted by the transcrystallinity model (Figs. A.1 and A.2). Obviously, both effects should have been responsible for the experimental observations, but it can be concluded

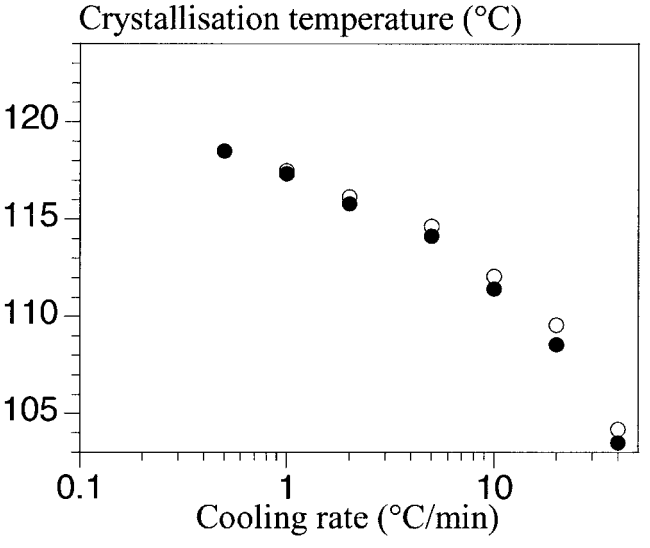

Figure A.2 Crystallization temperature versus cooling rate in (●) a 860 μm thick and in (○) a 200 μm-thick sample, with thermal gradient within the sample (no transcrystallinity) taken into account.

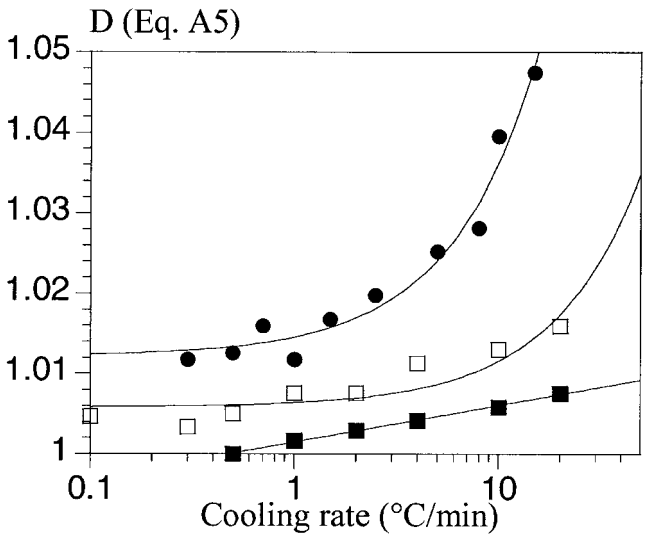

Figure A.3 Evolution of the *D* ratio [eq. (A.5)] as a function of cooling rate. Comparison between the effects of the (■) thermal gradient inside the sample alone, (□) transcrystallinity alone, and (●) experimental observations.

that transcrystallinity caused a much more disturbing effect than did the thermal gradient across the sample.

With regard to thermal resistance and, consequently, the thermal gradient between the sample and the furnace, we only can assume that our experimental protocol for calibration ensured that its effect was minimized.

In any case, if our experimental observations were due to this thermal gradient, they should have appeared on all measurements on polymer crystallization (as thermal properties are quite equivalent even if different). This was certainly not the case.

References

1. Fitchmun, D. R.; Newman, S. J Polym Sci, Part A-2: Polym Phys 1970, 8, 1545.
2. Gray, D. G. J Polym Sci. Polym Lett Ed 1974, 12, 509.
3. Campbell, D.; Qayyum, M. M. J Polym Sci. Polym Phys Ed 1980, 18, 83.
4. Lee, Y. C.; Porter, R. S. Polym Eng Sci 1986, 26, 633.
5. Chatterjee, A. M.; Price, F. P. J Polym Sci. Polym Phys Ed 1975, 13, 2369.
6. Chatterjee, A. M.; Price, F. P. J Polym Sci. Polym Phys Ed 1975, 13, 2391.
7. Fraser, G. V.; Keller, A.; Odell, J. A. J Appl Polym Sci 1978, 22, 2979.
8. Kamal, M. R.; Chu, E. Polym Eng Sci 1983, 23, 27.
9. Janeschitz-Kriegl, H. Progr Colloid Polym Sci 1992, 87, 117.
10. Billon, N.; Magnet, C.; Haudin, J. M.; Lefebvre, D. Colloid Polym Sci 1994, 272, 633.
11. Ozawa, T. Polymer 1971, 12, 150.
12. Billon, N.; Haudin, J. M. In Structure Development During Polymer Processing; Cunha, A. M.; Fakirov, S. Eds.; 2000; NATO Science Series, Serie E, Applied Sciences, Vol. 370; Kluwer: Dordrecht, p 113.
13. Wu, C. H.; Eder, G.; Janeschitz-Kriegl, H. Colloid Polym Sci 1993, 271, 1116.
14. Billlon, N. Ph.D. Thesis, Ecole Nationale Supérieure des Mines de Paris, 1987.
15. Billon, N.; Haudin, J. M. Colloid Polym Sci 1989, 267, 1064.
16. Billon, N.; Haudin, J. M. Ann Chim Fr 1990, 15, 249.
17. Haudin, J. M.; Billon, N. Prog Colloid Polym Sci 1992, 87, 132.
18. Evans, U. R. Trans Faraday Soc 1945, 41, 365.
19. Billon, N.; Haudin, J. M. J Therm Anal 1994, 42, 679.
20. Billon, N.; Barq, Ph.; Haudin, J. M. Intern Polym Process 1991, 6, 348.
21. (a) Avrami, M. J Chem Phys 1939, 7, 1103; (b) J Chem Phys 1940, 8, 212; (c) J Chem Phys 1941, 9, 177.
22. Keith, H. D.; Padden, F. J., Jr. Polymer 1984, 2, 28.
23. Hoffman, J. D.; Frolen, L. J.; Ross, G. S.; Lauritzen, J. I., Jr. J Res Natl Bur Stand Sect A 1975, 79A, 671.
24. Billon, N.; Henaff, V.; Haudin, J. M. J Appl Polym Sci 2002, 86, 734.